

the modulated exhaust motor<sup>5</sup> and by NWC with the T-burner.<sup>6</sup> It can be seen that the magnetic flow meter burner gives results similar to the T-burner and, in fact, gives a better fit to a standard response function curve. With NWR-11 a very noisy  $u(t)$  signal was observed, resulting in noisy  $u'(t)$  signals where the forced oscillation is only weakly visible. This led to a lower quality in the data reduction in terms of  $R_p$  and  $\alpha$ . This may be because NWR-11 contains a large portion of coarse AP (50% by weight of 400  $\mu\text{m}$ ), which may result in increased flow turbulence near the propellant surface registering as broadband noise by the magnetic flow meter.

### Conclusions

The addition of an ultrasound transducer for measuring the location of the propellant surface relative to the velocity measurement station and the use of a larger diameter propellant strand improved the ability of the magnetic flow meter to provide accurate data for the determination of a solid propellant pressure-coupled response. The use of an acoustic analysis in combination with the measurements allowed the use of data taken over a period of time, improving the accuracy of the calculated response and improving repeatability.

### Acknowledgments

The authors would like to acknowledge F. Blomshield of the Naval Air Warfare Center for his efforts in exchanging the NWR-11 propellant as part of the MWDDEA 5660 between the U.S. and France, and P. Kuentzmann and G. Lengellé of the Energetics Department at ONERA for helping to make possible the sabbatical year of M. Micci at ONERA.

### References

- 1Micci, M. M., "Workshop Report: Methods for Measuring Solid Propellant Combustion Response," 23rd JANNAF Combustion Meeting, Chemical Propulsion Information Agency Publication 457, Vol. 1, Oct. 1986.
- 2Wilson, J. R., and Micci, M. M., "Direct Measurement of High Frequency Solid Propellant Pressure-Coupled Admittances," *Journal of Propulsion and Power*, Vol. 3, No. 4, 1987, pp. 296-302.
- 3Shercliff, J. A., *Theory of Electromagnetic Flow-Measurement*, Cambridge Univ. Press, New York, 1962.
- 4Traineau, J. C., and Kuentzmann, P., "Ultrasonic Measurements of Solid Propellant Burning Rates in Nozzleless Rocket Motors," *Journal of Propulsion and Power*, Vol. 2, No. 3, 1986, pp. 215-222.
- 5Cauty, F., personal communication, Châtillon, France, June 1991.
- 6Blomshield, F. S., Crump, J. E., Mathes, H. B., and Beckstead, M. W., "Stability Testing of Full Scale Tactical Motors," AIAA Paper 91-1954, June 1991.

## Magnetohydrodynamics of a Particulate Suspension

Ali J. Chamkha\*

Kuwait University, Safat, 13060 Kuwait

### Introduction

CHAMKHA<sup>1</sup> reported exact solutions for the steady hydromagnetic two-dimensional flow of a particle-fluid suspension past an infinite porous flat plate. In the model used,

Received Feb. 17, 1991; revision received May 25, 1993; accepted for publication June 20, 1993. Copyright © 1995 by the American Institute of Aeronautics and Astronautics, Inc. All rights reserved.

\*Assistant Professor, Department of Mechanical and Industrial Engineering, P.O. Box 5969, Member AIAA.

the particle phase was assumed stress-free. The purpose of this Note is to generalize the model used by Chamkha<sup>1</sup> to include particle-phase viscous effects.

The mathematical model employed herein represents a generalization of the original dusty-gas model discussed by Marble<sup>2</sup> to include particle-phase viscosity and magnetic field effects. Particle-phase viscosity can be used to model several effects. Among these are particle-particle interactions and Reynolds stresses resulting from using a continuum model to represent a cloud of discrete particles.<sup>3</sup>

### Governing Equations

Let  $x$  denote the coordinate parallel to the direction of the flow, and  $y$  the coordinate perpendicular to it. Let a uniform magnetic field be applied along the  $y$  axis. Far from the plate both phases are in equilibrium and moving with speed  $V_\infty$  in the  $x$  direction. At the plate surface uniform suction with speed  $V_0$  is applied to the fluid phase. The fluid phase is assumed incompressible and electrically conducting. The suspended particles are assumed electrically nonconducting and have a small volume fraction. In addition, the magnetic Reynolds number is assumed to be small and the induced magnetic field is neglected.

The modified dusty-gas model to be employed herein can be written as

$$\begin{aligned} -V_0 \partial_y u &= \nu \partial_{yy} u + N \rho_p / \rho (u_p - u) + \sigma B_0^2 / \rho (V_\infty - u) \\ -V_0 \partial_y u_p &= \nu_p \partial_{yy} u_p + N(u - u_p) \end{aligned} \quad (1)$$

where  $\rho$ ,  $u$ , and  $\nu$  are the fluid-phase density, velocity in the  $x$  direction, and kinematic viscosity, respectively.  $\rho_p$ ,  $u_p$ , and  $\nu_p$  are the particulate-phase insuspension density (mass of particles per unit volume of suspension), velocity in the  $x$  direction, and kinematic viscosity, respectively.  $\sigma$ ,  $B_0$ , and  $N$  are the electrical conductivity, the magnetic induction, and the interphase force coefficient, respectively. In the present work the coefficients  $\rho$ ,  $\rho_p$ ,  $\nu$ ,  $\nu_p$ ,  $N$ , and  $B_0$  will all be treated as constants.

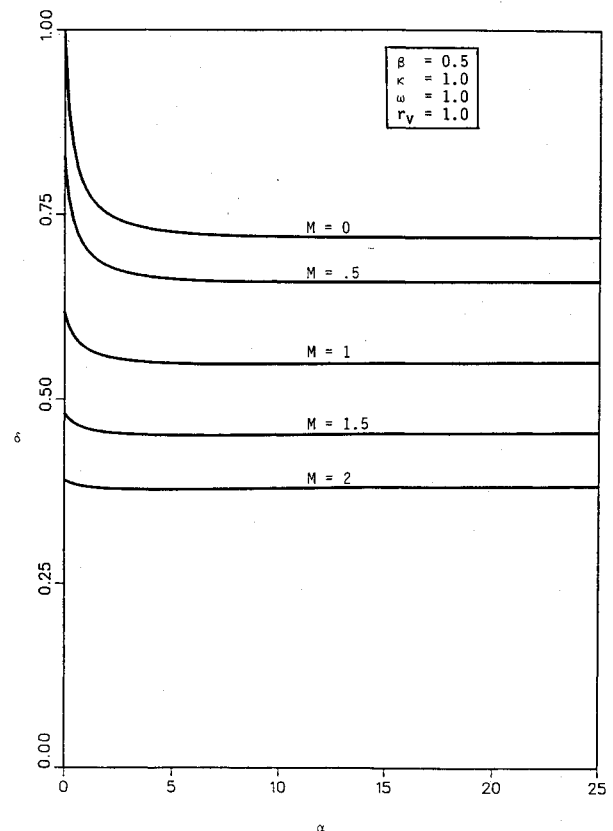


Fig. 1 Fluid-phase displacement thickness vs  $\alpha$ .

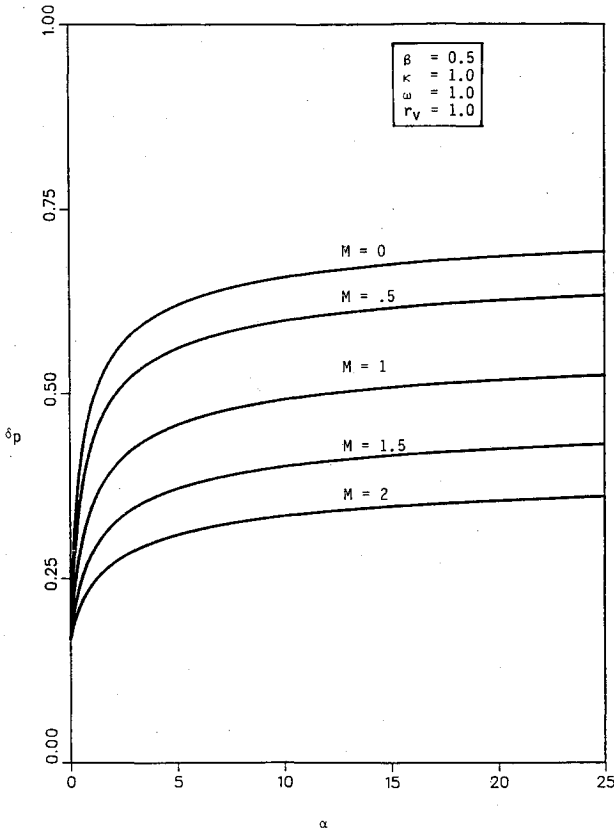


Fig. 2 Particle-phase displacement thickness vs  $\alpha$ .

Equations (1) can be made dimensionless by substituting

$$y = \nu\eta/V_\infty, \quad u = V_\infty F(\eta), \quad u_p = V_\infty F_p(\eta) \quad (2)$$

to give the coupled differential equations

$$\begin{aligned} F'' + r_v F' + \kappa\alpha(F_p - F) - M^2(F - 1) &= 0 \\ \beta F_p'' + r_v F_p' + \alpha(F - F_p) &= 0 \end{aligned} \quad (3)$$

where a prime denotes ordinary differentiation with respect to  $\eta$  and

$$\begin{aligned} r_v = V_0/V_\infty, \quad \alpha = N\nu/V_\infty^2, \quad \beta = \nu_p/\nu \\ \kappa = \rho_p/\rho, \quad M = \sqrt{\sigma/(\rho\nu)}B_0\nu/V_\infty \end{aligned} \quad (4)$$

are the suction parameter, the inverse Stokes number, the viscosity ratio, the particle loading, and the Hartmann number, respectively.

The displacement thicknesses and the skin friction coefficients for both the fluid and particle phases are defined, respectively

$$\begin{aligned} \delta = \int_0^\infty (1 - F) d\eta, \quad \delta_p = \int_0^\infty (1 - F_p) d\eta \\ C_f = F'(0), \quad C_{fp} = \beta\kappa F_p'(0) \end{aligned} \quad (5)$$

where the factor  $\beta\kappa$  in Eq. (5d) reflects that both  $C_f$  and  $C_{fp}$  are made dimensionless using the fluid-phase density and kinematic viscosity. Thus,  $C_{fp}/C_f$  is the ratio of the actual shear stresses.

### Results

For an inviscid particle phase, Eq. (3) (with  $\beta = 0$ ) is solved subject to

$$F(0) = 0, \quad F(\infty) = 1, \quad F_p(\infty) = 1 \quad (6)$$

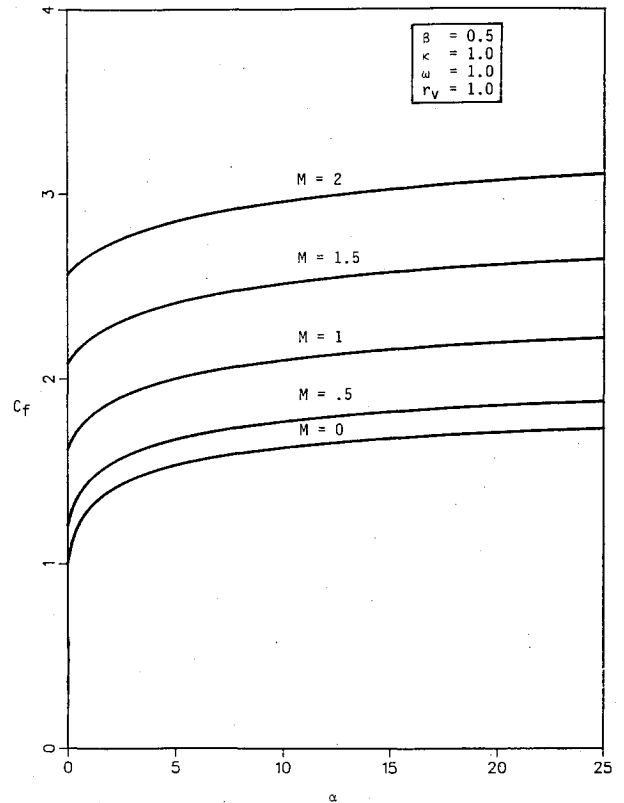


Fig. 3 Fluid-phase skin friction coefficient vs  $\alpha$ .

in a previous paper by the present author. Attention will, therefore, be focused herein on the case of  $\beta \neq 0$ .

When  $\beta \neq 0$  (viscous particle phase), an additional boundary condition on  $F_p$  at the wall is needed. While the exact form of the boundary conditions to be satisfied by the particulate phase at a solid surface is poorly understood at present, two tentative conditions are used as follows:

$$F_p(0) = F_{p0}, \quad F_p'(0) = \omega F_p(0) \quad (7)$$

where  $\omega$  is a constant. In Eq. (7a)  $F_{p0}$  is a dimensionless wall slip velocity of the particle phase. Equation (7b) (suggested by Soo<sup>4</sup>) can be recognized as similar to the slip condition employed in rarefied gas dynamics. Obviously, if  $F_{p0} = 0$  or  $\omega = \infty$ , a no-slip condition is recovered.

Equations (3a) and (3b) can be combined into a fourth-order, linear, nonhomogeneous, ordinary differential equation for  $F_p$ . This can be written as

$$\begin{aligned} \beta F_p^{IV} + r_v(1 + \beta)F_p^{III} + [r_v^2 - M^2\beta - \alpha(1 + \kappa\beta)]F_p'' \\ - r_v[M^2 + \alpha(1 + \kappa)]F_p' + M^2\alpha F_p = M^2\alpha \end{aligned} \quad (8)$$

Equation (8) is solved subject to Eqs. (6) and (7a) to yield

$$F_p = 1 - C_1 \exp(-\lambda_1 \eta) - C_2 \exp(-\lambda_2 \eta) \quad (9)$$

where  $\lambda_1$  and  $\lambda_2$  are the absolute values of the two negative roots of the equation

$$\begin{aligned} \beta\lambda^4 + r_v(1 + \beta)\lambda^3 + [r_v^2 - M^2\beta - \alpha(1 + \kappa\beta)]\lambda^2 \\ - r_v[M^2 + \alpha(1 + \kappa)]\lambda + M^2\alpha = 0 \end{aligned} \quad (10)$$

where

$$\begin{aligned} C_1 = [1 + B(1 - F_{p0})]/\{[r_v(\lambda_2 - \lambda_1) \\ - \beta(\lambda_2^2 - \lambda_1^2)]/\alpha\} \\ B = 1 + (r_v\lambda_2 - \beta\lambda_2^2)/\alpha, \quad C_2 = C_1 + 1 - F_{p0} \end{aligned} \quad (11)$$

It should be mentioned that the acceptable physical solution of Eq. (10) is having two negative and two positive roots. No way was found to prove that analytically. However, in all of the numerical examples considered subsequently, this condition was satisfied.

Differentiating  $F_p$  from Eq. (9) twice and substituting into Eq. (3b) and solving for  $F$  yield

$$F = 1 - AC_1 \exp(-\lambda_1 \eta) - BC_2 \exp(-\lambda_2 \eta) \quad (12)$$

where

$$A = 1 + (r_v \lambda_1 - \beta \lambda_1^2) / \alpha \quad (13)$$

The corresponding expressions for  $\delta$ ,  $\delta_p$ ,  $C_f$ , and  $C_{fp}$  can be shown to be

$$\begin{aligned} \delta &= AC_1 / \lambda_1 + BC_2 / \lambda_2, & \delta_p &= C_1 / \lambda_1 + C_2 / \lambda_2 \\ C_f &= \lambda_1 AC_1 + \lambda_2 BC_2, & C_{fp} &= \beta \kappa (\lambda_1 C_1 + \lambda_2 C_2) \end{aligned} \quad (14)$$

If Eq. (7b) is employed instead of Eq. (7a), the same solutions result with  $C_1$  and  $C_2$  are, respectively, replaced by  $C_3$  and  $C_4$ , where

$$\begin{aligned} C_4 &= \lambda_1 [1 + \omega(\beta \lambda_1 - r_v) / \alpha] / [(\omega \\ &+ \lambda_1) B - (\omega + \lambda_2) A] \\ C_3 &= [\omega + C_4(\omega + \lambda_2)] / (\omega + \lambda_1) \end{aligned} \quad (15)$$

All of the results reported herein reduce to those reported earlier by Chamkha and Peddieson<sup>5</sup> if  $M$  is equated to zero.

A selective set of results based on the numerical evaluation of the solutions obtained by using Eq. (7b) is presented in Figs. 1–4. These figures illustrate the behavior of the fluid-phase displacement thickness  $\delta$ , the particle-phase displacement

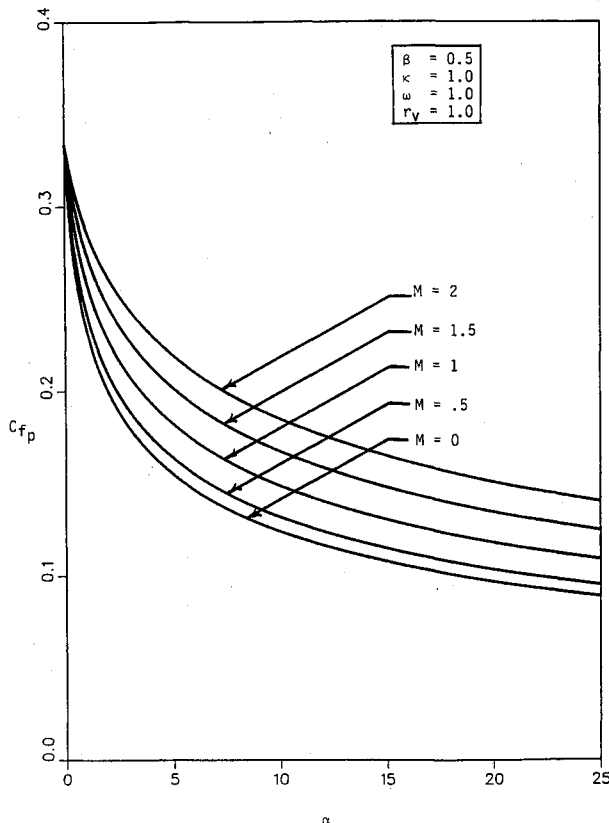


Fig. 4 Particle-phase skin friction coefficient vs  $\alpha$ .

Table 1 Corresponding values as  $\alpha \rightarrow \infty$

$M$	$\delta$	$\delta_p$	$C_f$	$C_{fp}$
0	0.74177	0.74082	1.94780	0.17413
0.5	0.68218	0.68124	2.11400	0.01886
1.0	0.57294	0.57200	2.50620	0.02225
1.5	0.47704	0.47612	2.99410	0.02641
2.0	0.40338	0.40247	3.52100	0.03085

thickness  $\delta_p$ , the fluid-phase skin friction coefficient  $C_f$ , and the particle-phase skin friction coefficient vs the inverse Stokes number  $\alpha$  for various values of the Hartmann number  $M$ , respectively. Increases in  $M$  have the tendency to decrease the region close to the wall where deviations from uniformity occur. This, in turn, causes the slope at the wall to increase. This is reflected in the increases in  $C_f$  and  $C_{fp}$  and the decreases in  $\delta$  and  $\delta_p$  observed from Figs. 1–4 as  $M$  increases. Table 1 shows the values of  $\delta$ ,  $\delta_p$ ,  $C_f$ , and  $C_{fp}$  as  $\alpha \rightarrow \infty$ .

### Conclusions

A continuum two-phase (particle-fluid) model allowing for particle-phase stresses and magnetic field effects is developed and applied to the problem of flow of a dusty gas (or fluid) past an infinite porous flat plate. Analytical solutions of this model are reported and some graphical results are presented and discussed. It is found that both the fluid and particle displacement thicknesses decrease while both the fluid and particle skin friction coefficients increase as the Hartmann number increases.

### References

- Chamkha, A. J., "Exact Solutions for Hydromagnetic Flow of a Particulate Suspension," *AIAA Journal*, Vol. 30, No. 7, 1992, pp. 1922–1924.
- Marble, F. E., "Dynamics of Dusty Gases," *Annual Review of Fluid Mechanics*, Vol. 2, No. 1, 1970, pp. 397–446.
- Drew, D. A., "Mathematical Modeling of Two-Phase Flow," *Annual Review of Fluid Mechanics*, Vol. 15, No. 1, 1983, pp. 261–291.
- Soo, S. L., "Development of Theories of Liquid-Solid Flow," *Journal of Pipelines*, Vol. 4, No. 1, 1984, pp. 137–142.
- Chamkha, A. J., and Peddieson, J., "Exact Solutions for the Two-Phase Asymptotic Suction Profile," *Developments in Theoretical and Applied Mechanics*, Vol. 14, No. 1, 1988, pp. 215–222.

## Effects of Initial Boundary Layers to the Lobed Mixer Trailing Streamwise Vorticity

Simon C. M. Yu,\* X. G. Xu,† and T. H. Yip†  
Nanyang Technological Institute, 2263, Singapore

### Nomenclature

- $C_l$  = normalized streamwise circulation,  $\Gamma_s / U_r h \tan \varepsilon$   
 $C_T$  = normalized streamwise circulation at the trailing edge based on the analysis of Ref. 4  
 $h$  =  $\lambda$  lobe height, 33 mm

Received June 29, 1995; revision received Oct. 15, 1995; accepted for publication Oct. 31, 1995. Copyright © 1995 by the American Institute of Aeronautics and Astronautics, Inc. All rights reserved.

\*Lecturer, Thermal and Fluids Engineering Division, School of Mechanical and Production Engineering, Member AIAA.

†Research Student, Thermal and Fluids Engineering Division, School of Mechanical and Production Engineering.